

# Conifers exhibit a characteristic inactivation of auxin to maintain tissue homeostasis

Federica Brunoni<sup>1,2,4</sup> , Silvio Collani<sup>1</sup> , Rubén Casanova-Sáez<sup>2</sup> , Jan Šimura<sup>2</sup> , Michal Karady<sup>2,5</sup> , Markus Schmid<sup>1</sup> , Karin Ljung<sup>2</sup>  and Catherine Bellini<sup>1,3</sup> 

<sup>1</sup>Umeå Plant Science Centre, Department of Plant Physiology, Umeå University (Umu), 90736, Umeå, Sweden; <sup>2</sup>Umeå Plant Science Centre, Department of Forest Genetics and Plant Physiology, Swedish University of Agricultural Sciences (SLU), 90183, Umeå, Sweden; <sup>3</sup>Institut Jean-Pierre Bourgin, INRAE, AgroParisTech, Université Paris-Saclay, 78000, Versailles, France; <sup>4</sup>Present address: Laboratory of Growth Regulators, Faculty of Science, Palacký University & Institute of Experimental Botany, The Czech Academy of Sciences, Šlechtitelů 27, CZ-78371, Olomouc, Czech Republic; <sup>5</sup>Present address: Department of Chemical Biology and Genetics, Faculty of Science, Centre of the Region Haná for Biotechnological and Agricultural Research, Palacký University, CZ-78371, Olomouc, Czech Republic

## Summary

Authors for correspondence:

Catherine Bellini

Tel: +46 90 786 96 24

Email: catherine.bellini@umu.se

Karin Ljung

Tel: +46 90 786 83 55

Email: karin.ljung@slu.se

Received: 17 December 2019

Accepted: 27 January 2020

New Phytologist (2020) 226: 1753–1765

doi: 10.1111/nph.16463

**Key words:** auxin conjugates, auxin homeostasis, conifers, *GH3* genes, indole-3-acetic acid (IAA), *Picea abies*.

- Dynamic regulation of the concentration of the natural auxin (IAA) is essential to coordinate most of the physiological and developmental processes and responses to environmental changes. Oxidation of IAA is a major pathway to control auxin concentrations in angiosperms and, along with IAA conjugation, to respond to perturbation of IAA homeostasis. However, these regulatory mechanisms remain poorly investigated in conifers. To reduce this knowledge gap, we investigated the different contributions of the IAA inactivation pathways in conifers.
- MS-based quantification of IAA metabolites under steady-state conditions and after perturbation was investigated to evaluate IAA homeostasis in conifers. Putative *Picea abies* *GH3* genes (*PaGH3*) were identified based on a comprehensive phylogenetic analysis including angiosperms and basal land plants. Auxin-inducible *PaGH3* genes were identified by expression analysis and their IAA-conjugating activity was explored.
- Compared to Arabidopsis, oxidative and conjugative pathways differentially contribute to reduce IAA concentrations in conifers. We demonstrated that the oxidation pathway plays a marginal role in controlling IAA homeostasis in spruce. By contrast, an excess of IAA rapidly activates *GH3*-mediated irreversible conjugation pathways.
- Taken together, these data indicate that a diversification of IAA inactivation mechanisms evolved specifically in conifers.

## Introduction

The phytohormone auxin mediates a variety of different developmental processes during a plant's life cycle, acting also as an inter-cellular signal integrating environmental inputs and growth responses. An important level of regulation in auxin responses is the establishment of concentration gradients between cells and tissues (Vanneste & Friml, 2009; Ljung, 2013). Thus, it is critical for plants to tightly control differential auxin distribution, both at spatial and at temporal levels. Metabolic and transport mechanisms jointly generate auxin gradients within tissues (Ruiz Rosquete *et al.*, 2012; Ljung, 2013). Auxin transport depends on the differential localisation of influx and efflux carriers at the plasma membrane, providing the plant with a carrier-driven mechanism that controls auxin directionality and distribution within tissues (Vanneste & Friml, 2009). Additionally, auxin concentrations are regulated via the balance between the rates of auxin biosynthesis and auxin inactivation, extending the complexity of the regulatory network of cellular auxin homeostasis (Ljung, 2013;

Kramer & Ackelsberg, 2015). The predominant auxin found in plants is IAA. Multiple auxin biosynthetic pathways that rely on tryptophan (Trp) as a precursor have been proposed. The elucidation of these biosynthetic pathways demonstrated that IAA is locally produced and not ubiquitously, as it was earlier assumed (LeClere *et al.*, 2002; Normanly, 2010; Zhao, 2018). There is also evidence for a Trp-independent pathway for IAA biosynthesis but this pathway is less well understood (Ljung, 2013; Zhao, 2018). Reduction of the cellular concentrations of free IAA also relies on auxin inactivation mechanisms, such as conjugation and degradation. IAA can be conjugated to various amino acid, peptide and sugar moieties. Auxin conjugates might function as short-term intermediates that can release free IAA upon hydrolysis when required (LeClere *et al.*, 2002; Ludwig-Müller, 2011). IAA can be reversibly conjugated via ester linkages to glucose by UDP-glucosyl transferases to produce indole-3-acetyl-1-glucosyl ester (IAGlc) (Jackson *et al.*, 2001). Members of the GRETCHEN HAGEN3 (*GH3*) family of acyl amido synthetases mediate conjugation of IAA with amino acids (Staswick

*et al.*, 2005; Westfall *et al.*, 2011). IAA amino acid conjugates are regarded as either reversible or irreversible IAA metabolites based on *in vitro* activity and *in planta* feeding assays (Östin *et al.*, 1998; Kowalczyk & Sandberg, 2001). Conjugation to particular moieties, such as aspartate (Asp) and glutamate (Glu) to produce indole-3-acetyl-L-aspartic acid (IAA<sub>Asp</sub>) and indole-3-acetyl glutamic acid (IAGlu), seems to lead to degradation (Östin *et al.*, 1998; Tam *et al.*, 2000), whereas IAA conjugates with other amino acids (e.g. alanine, leucine or phenylalanine) are transient storage compounds that could be hydrolysed back to free IAA via auxin amino acid conjugate hydrolases (Kowalczyk & Sandberg, 2001; LeClere *et al.*, 2002). The oxidation of IAA to oxindole-3-acetic acid (oxIAA) is one of the major catabolic pathways to inactivate auxin (Östin *et al.*, 1998; Peer *et al.*, 2013; Pěnčík *et al.*, 2013). Recent findings have demonstrated that the DIOXYGENASE FOR AUXIN OXIDATION (DAO) protein, a 2-oxoglutarate-dependent-Fe(II) dioxygenase (2OGD), catalyses conversion of IAA to oxIAA (Zhao *et al.*, 2013; Porco *et al.*, 2016; Zhang *et al.*, 2016). oxIAA can be further glucosylated to oxindole-3-acetyl-1-glucosyl ester (oxIAGlc) (Östin *et al.*, 1998; Kai *et al.*, 2007). The characterisation of these metabolic pathways together with the identification of the key components of the auxin conjugation and degradation machineries have significantly improved our understanding of their respective contribution to the regulation of auxin homeostasis. For example, metabolic profiling of the loss-of-function *dao1* mutant showed that, despite the reduction of oxIAA concentration in the mutant, no significant accumulation of IAA was observed (Porco *et al.*, 2016). Interestingly, the concentrations of IAA conjugates, such as IAA<sub>Asp</sub> and IAGlu, were found to be much higher in the *dao1* mutant than in wild-type plants and the accumulation of these IAA metabolites was associated with an increase of *GH3* gene expression in the *dao1* mutant (Porco *et al.*, 2016). These findings demonstrated that *DAO1* acts in concert with *GH3* genes to maintain optimal auxin concentrations, and thus the regulation of IAA homeostasis by these auxin inactivation pathways is redundant (Stepanova & Alonso, 2016; Zhang & Peer, 2017). Additionally, differences in enzyme kinetics and expression levels between DAO and GH3 have suggested that DAO, having much slower enzyme kinetics compared with GH3 proteins, contributes to maintain constitutively basal auxin concentrations under normal growth conditions, while GH3 rapidly responds to environmental factors that increase cellular IAA concentrations (Mellor *et al.*, 2016; Stepanova & Alonso, 2016). Although the majority of knowledge about auxin metabolism is based on studies in *Arabidopsis thaliana*, the conjugation and oxidation mechanisms also appear to be present in many other species (Sztejn *et al.*, 1999; Cooke *et al.*, 2002; Ludwig-Müller, 2011; Zhang & Peer, 2017). Analysis of endogenous IAA metabolites in cyanobacteria, algae and bryophytes revealed that free IAA and its primary catabolite oxIAA contribute the most to the total auxin pool in these species (Drábková *et al.*, 2015; Žižková *et al.*, 2017). The concentration of IAA<sub>Asp</sub> was close to the detection limit in algae and cyanobacteria under normal growth conditions, while exogenous application of radiolabelled IAA led to accumulation of IAA<sub>Asp</sub> and IAGlc in green algae (Žižková *et al.*, 2017).

IAA amino acid conjugates were not abundant in bryophytes and only IAA<sub>Asp</sub> and IAGlu were detected in some species, if present at all (Drábková *et al.*, 2015). Ester-linked conjugates, such as IAGlc and oxIAGlc, were also present in liverworts and mosses but they did not contribute considerably to the total pool of auxin (Drábková *et al.*, 2015). In gymnosperms, it has been postulated that the two different categories of IAA conjugates have a different function during early growth of Scots pine (*Pinus sylvestris*) seedlings (Ljung *et al.*, 2001). Ester-linked conjugates of IAA were hydrolysed during seed germination acting as a source for release of free IAA, while IAA<sub>Asp</sub>, together with oxIAA, contributed less to the IAA pool size in the seed but progressively accumulated during initial seedling growth (Ljung *et al.*, 2001). These findings suggest that flowering plants did not evolve *de novo* mechanisms for the homeostatic control of the IAA pool size, but have rather developed mechanisms from metabolic pathways that were already present in the early land plants and algae.

However, the function of these processes and the study of specific enzymes catalysing these reactions in nonmodel species remain poorly understood. Until recently, this information was inaccessible due to unavailable genomic resources and the lack of suitable tools for the quantification of auxin metabolites. The release of draft genomes from *Picea abies*, *Picea glauca* and *Pinus taeda* (Birol *et al.*, 2013; Nystedt *et al.*, 2013; Neale *et al.*, 2014; Zimin *et al.*, 2014), combined with the development of sensitive methods for the identification and quantification of auxin metabolites, have opened new possibilities for functional studies regarding IAA homeostatic mechanisms in conifers. This article provides strong evidence that the formation of oxIAA does not contribute considerably to maintain IAA homeostasis in Norway spruce (*P. abies*), as well as in other conifers such as Scots pine and lodgepole pine (*Pinus contorta*) in contrast to *Arabidopsis*. Besides, the irreversible conversion of IAA to IAA<sub>Asp</sub> and IAGlu seems to act constitutively in steady-state conditions and to be the main pathway induced in response to perturbation of the IAA content, to maintain IAA homeostasis in conifers. We also report the identification of auxin-inducible Norway spruce Group II members of the *GH3* family and confirm that the corresponding recombinant proteins catalyse the conjugation of IAA with Asp and/or Glu. In addition, we demonstrate that no functional orthologues to angiosperm DAOs could be identified in Norway spruce indicating that, in contrast to *Arabidopsis*, the oxidative catabolism of IAA is unlikely to be mediated by DAO-like enzymes. Together, our data suggest that at least part of the sophisticated regulatory machinery controlling IAA homeostasis is conserved in conifers and that the respective contribution of the oxidative and conjugation pathways is different compared to angiosperms. This suggests a diversification of the homeostatic control of IAA in gymnosperms.

## Materials and Methods

### Plant material and growth conditions

Norway spruce seeds (*P. abies* L. Karst) were provided by Sveaskog (Lagan, Sweden) and pine seeds (*P. sylvestris* L. and

*P. contorta* Dougl.) were provided by SkogForsk (Sävar, Sweden). Seeds were soaked in tap water for 12 h at 4°C and then sown in fine wet vermiculite. Germination and growth of seedlings occurred in a growth chamber at a light intensity of  $150 \mu\text{mol m}^{-2} \text{s}^{-1}$  under long-day conditions (16 h : 8 h, light : dark). Temperatures were set to 22°C during the day and 18°C during the night.

#### IAA metabolite profiling and feeding experiment with unlabelled and labelled IAA

Spruce and pine seedlings were sampled 14 d after sowing, and dissected organs (cotyledons, hypocotyl and root) were collected in four independent replicates (10 mg of tissue per sample). For feeding experiments with unlabelled IAA, 2-wk-old spruce and pine seedlings were first cultured in flasks containing 50 ml of half-strength ( $\frac{1}{2}$ ) Murashige–Skoog (MS; Duchefa, Harleem, the Netherlands) liquid medium for 24 h under gentle shaking and in darkness. Liquid cultures were subsequently supplemented with 10  $\mu\text{M}$  IAA for 0, 6 and 24 h under gentle shaking and in darkness. Mock-treated seedlings were used as controls. For each time point, 10 mg of roots was collected in four independent replicates. For feeding experiments with labelled IAA, 2-wk-old spruce seedlings were first incubated in  $\frac{1}{2}$ MS liquid medium for 24 h under gentle shaking and in darkness. Liquid cultures were subsequently supplemented with 10  $\mu\text{M}$  [ $^{13}\text{C}_6$ ]-IAA for 0, 6 and 24 h under gentle shaking and in darkness. For each time point, 10 mg of spruce roots was collected in five independent replicates. The extraction, purification and LC-MS/MS analysis of endogenous concentrations of auxin and its metabolites were carried out according to Novák *et al.* (2012). Briefly, c. 10 mg of frozen material per sample was homogenised using a bead mill (27 Hz, 10 min, 4°C; MixerMill, Retsch GmbH, Haan, Germany) and extracted in 1 ml of 50 mM sodium phosphate buffer containing 1% sodium diethyldithiocarbamate and a mixture of  $^{13}\text{C}_6$ - or deuterium-labelled internal standards. After centrifugation (20 000 g, 15 min, 4°C), the supernatant was transferred into new Eppendorf tubes. pH was then adjusted to 2.5 by 1 M HCl and applied on preconditioned solid-phase extraction columns (Oasis HLB, 30 mg of 1 ml; Waters Inc., Milford, MA, USA). After sample application, the column was rinsed with 2 ml 5% methanol. Compounds of interest were then eluted with 2 ml 80% methanol. MS analysis and quantification were performed using an LC-MS/MS system consisting of a 1290 Infinity Binary LC System coupled to a 6490 Triple Quad LC/MS System with Jet Stream and Dual Ion Funnel technologies (Agilent Technologies, Santa Clara, CA, USA).

#### Sequences and phylogenetic analysis

The gene family information available in PlantGenIE (<https://plantgenie.org>; Sundell *et al.*, 2015) was used to retrieve putative GH3 genes from the *P. abies* genome. The same procedure was adopted to retrieve GH3-like protein sequences also from *P. taeda* and nonseed plants, such as *Selaginella moellendorffii* and *Physcomitrella patens*. The GH3 protein sequences from *Oryza sativa*, *Populus trichocarpa* and *Malus domestica* were downloaded

from PHYTOZOME v.12.1 (<https://phytozome.jgi.doe.gov/pz/portal.html>; Goodstein *et al.*, 2012) and PlantGenIE. *A. thaliana* GH3 proteins were used to blast embryophyte and chlorophyte genomes in PHYTOZOME, allowing the selection of additional putative GH3 protein sequences from *Marchantia polymorpha* and *Sphagnum fallax*, as no GH3 sequences were found in chlorophytes.

The Arabidopsis DAO1 protein sequence was used as a query in BLASTP searches for predicted proteins with high confidence from *P. abies* and *P. taeda* genomes (*P. abies* and *P. taeda* v.1.0, <http://congenie.org/>; Nystedt *et al.*, 2013; Zimin *et al.*, 2014). AtDAO1 protein was used to blast embryophyte and chlorophyte genomes in PHYTOZOME, allowing the selection of putative 2OGD protein sequences from *S. moellendorffii*, *P. patens*, *Coccomyxa subellipsoidea*, *Micromonas pusilla*, *Ostreococcus lucimarinus*, *Volvox carteri*, *Dunaliella salina* and *Chlamydomonas reinhardtii*. The DAO protein sequences of *O. sativa*, *P. trichocarpa* and *M. domestica* were retrieved from PHYTOZOME and GenBank (National Center for Biotechnology Information; <https://www.ncbi.nlm.nih.gov/genbank/>).

Multiple sequence alignment was performed using MUSCLE (Edgar, 2004) as implemented in MEGA6 (<http://megasoftware.net/>; Tamura *et al.*, 2013) under default parameters. Phylogenetic trees were reconstructed with the neighbor-joining method (Saitou & Nei, 1987) in MEGA6 with 1000 bootstrap iterations. Evolutionary distances were computed using the Dayhoff matrix-based method (Schwarz & Dayhoff, 1979) and are reported in number of amino acid substitutions per site.

#### RNA isolation and real-time PCR

Root samples for analysing the mRNA levels of *PaGH3s* in response to auxin were collected from spruce seedlings that were cultured in flasks containing 50 ml of  $\frac{1}{2}$ MS liquid medium supplemented with 10  $\mu\text{M}$  IAA for 0 or 6 h under gentle shaking and in darkness. Mock-treated seedlings were used as a control. Samples were frozen in liquid nitrogen and stored at  $-80^\circ\text{C}$  after collection. Total RNA was isolated using the Spectrum Plant Total RNA kit (Sigma-Aldrich) according to the manufacturer's instructions. For each sample, 1  $\mu\text{g}$  of total RNA was reverse transcribed with an iScript cDNA Synthesis Kit (Bio-Rad) according to the manufacturer's instructions. Quantitative real-time PCR (qRT-PCR) was performed on a CFX384 Touch Real-Time PCR Detection System (Bio-Rad) using 20 $\times$  LightCycler 480 SYBR Green I Master (Roche). The three step cycling programme was as follows: 95°C for 3 min, followed by 40 cycles at 95°C for 10 s, 60°C for 15 s and 72°C for 30 s. Melting curve analysis was conducted between 65 and 95°C. The specificity of the PCR products was confirmed by analysing melting curves and sequencing. Only primer pairs that produced a linear amplification and qPCR products with a single-peak melting curve were used for further analysis. The efficiency of each pair of primers was determined from the amplification cycle threshold ( $C_t$ ) plot with a serial dilution of mixed cDNA and the equation  $E = 10^{(-1/\text{slope})} - 1$ . The *P. abies* *eIF4A* gene (MA\_50378g0010) was used as a constitutive internal standard,

which showed no clear changes in Ct values, to normalise the obtained gene expression results. Expression levels were calculated using the  $\Delta\Delta C_t$  method (Pfaffl, 2001). Three biological replicates, each with three technical replicates, were performed for each test. Primer sequences are listed in Supporting Information Table S1.

#### 5'- and 3'-RACE, cloning, protein expression and enzyme assay

The full-length coding regions of *PaGH3s* (*PaGH3.16*, *PaGH3.17*, *PaGH3.gII.8*, *PaGH3.gII.9*) and *Pa2OGDs* (*Pa2OGD.1*, *Pa2OGD.2*, *Pa2OGD.6*, *Pa2OGD.8*) were obtained by combining incomplete gene annotation from the Norway spruce genome, with 5'- and 3'-RACE (rapid amplification of cDNA ends; Gene Racer Kit; Invitrogen), which was carried out according to the manufacturer's instructions. The full-length coding regions were then amplified by PCR from spruce cDNA template using gene-specific primers (Fig. S1; Table S1) with additional *Xba*I and *Hind*III or *Nhe*I sites required for *PaGH3s* or with additional *Nco*I and *Acc*65I sites required for *Pa2OGDs* to clone into the pETM11 expression vector. Plasmids expressing recombinant spruce proteins were transformed into *Escherichia coli* BL21 (DE3). Production of recombinant proteins was induced by the addition of 0.1 mM isopropyl-D-thiogalactopyranoside (IPTG). Cells were grown overnight at 20°C with constant shaking at 250 rpm. Protein expression was tested by Western blotting with anti-6x His antibody horseradish peroxidase (HPR) conjugate (Sigma A7058-1VL, 1: 10 000 dilution). IAA conjugation and oxidation assays were performed as described by Brunoni *et al.* (2019).

## Results

### IAA conjugation processes mostly control IAA homeostasis in conifer seedlings

To investigate how IAA is metabolised in conifers, basal IAA metabolism was analysed in three different conifer species under steady-state growth conditions. *P. abies*, *P. sylvestris* and *P. contorta* were chosen as they dominate the landscapes in Sweden and due to their ecological and economical relevance. Vermiculite-grown conifer seedlings were harvested 14 d after germination, and profiling of endogenous IAA metabolites was carried out in cotyledons, hypocotyl and root, separately. Figs 1 and S2 show IAA metabolite profiling in the different organs of spruce and pine seedlings, respectively. For all conifers, free IAA was abundant in roots while the concentration was lower in the cotyledons and hypocotyl and, together with IAGlc, contributed to most of the total auxin metabolite pool in both spruce and pine seedlings (Figs 1, S2). With regard to irreversible IAA catabolism, IAAsp and IAGlu were the most abundant IAA catabolites while oxIAA occurred at very low concentration in all spruce and pine organs analysed (Figs 1, S2). Interestingly, IAAsp and IAGlu were not equally distributed throughout the pine organs, with IAAsp contents close to limit of detection in the hypocotyl of *P. sylvestris* and IAGlu not detected in roots or close to the limit of detection in the hypocotyl

of *P. contorta* (Fig. S2). The glucosylester oxIAGlc is present at high concentrations in Arabidopsis seedlings (Kai *et al.*, 2007; Porco *et al.*, 2016) and was suggested to be synthesised via glucosylation of oxIAA and not oxidation of IAGlc (Tanaka *et al.*, 2014; Porco *et al.*, 2016). Compared to Arabidopsis seedlings (Porco *et al.*, 2016), oxIAGlc was found to be much less abundant in all conifer seedlings (Figs 1, S2). oxIAGlc was detected at low concentrations in all three organs from pine seedlings, but it was below the detection limit in cotyledons from spruce seedlings (Figs 1, S2). Together, these results suggest that, under steady-state conditions, the conjugation pathways are likely to be the main contributors to IAA homeostasis compared to the formation of oxIAA and oxIAGlc in conifers.

### Exogenous application of IAA rapidly activates the conjugation pathway in conifer roots

Application of IAA and generation of transgenic or mutated lines, in which the functionality of key regulators in auxin metabolism are affected, leads to perturbations of IAA homeostasis (Staswick *et al.*, 2005; Park *et al.*, 2007; Zhao *et al.*, 2013; Pěnčík *et al.*, 2013; Porco *et al.*, 2016). When mutant or transgenic lines are not easily available, as with spruce, metabolic analysis of IAA-treated plants represents a valid alternative to study the relative contribution of the different inactivation mechanisms to the regulation of IAA concentrations. When spruce seedlings were treated with 1 or 10  $\mu$ M of exogenous IAA, alteration in the concentrations of IAA metabolites was similar in the three different organs (cotyledons, hypocotyl and root), but more evident in root tissues (Fig. S3), and 10  $\mu$ M of IAA was the most effective concentration used (Fig. S3).

We then analysed the effect of disturbed IAA homeostasis by incubating 2-wk-old spruce and pine seedlings with 10  $\mu$ M IAA, and roots were harvested at 6 and 24 h after treatment. After 6 h, exogenous auxin application led to a strong endogenous IAA accumulation, but after 24 h free IAA levels decreased dramatically, reaching the basal concentrations detected in mock treatments, suggesting that the IAA inactivation machinery was activated within this time span (Figs 2a, S4). Activation of IAA metabolism occurred in all three species even after 6 h, and all IAA metabolites increased dramatically after treatment with exogenous IAA compared to the concentrations detected in mock treatments (Figs 2a, S4). Among the primary degradation products, IAAsp and IAGlu contents were much higher than oxIAA, and accumulated over time in spruce (Fig. 2a). IAA was more efficiently conjugated with Asp than with Glu, as much higher concentrations of IAAsp than IAGlu were measured (Fig. 2a). The content of the ester-linked conjugates IAGlc was also higher in IAA-treated seedlings than in mock-treated seedlings at 6 and 24 h, suggesting that glucosylation of IAA also contributed to the homeostatic regulation (Fig. 2a). After application of exogenous IAA, the amount of oxIAGlc also increased, but concentrations were >100-fold lower than IAGlc, confirming the marginal role of the oxidative pathways in homeostatic regulation of IAA in spruce (Fig. 2a). A similar metabolic pattern was observed in pine roots treated with exogenous auxin (Fig. S4).

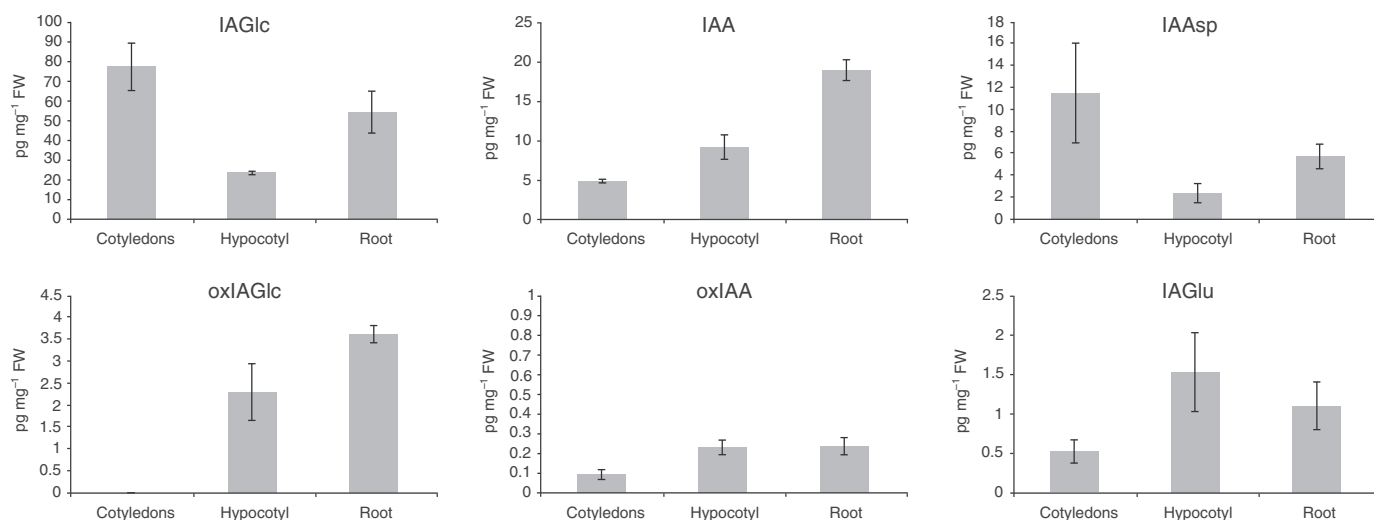


**Fig. 1** Levels of IAA metabolites in different organs of *Picea abies* seedlings. IAA and IAA metabolites oxIAA, oxIAGlc, IAGlc, IAAsp and IAGlu were quantified in cotyledons, hypocotyl and root from 2-wk-old spruce seedlings. The concentration of oxIAGlc in cotyledons was under the detection limit of the LC-MS/MS method used. The concentrations of all metabolites are in picograms per milligram fresh weight (FW). Error bar indicates  $\pm$  SD ( $n = 4$ ). See Supporting Information Fig. S2 for IAA profiling from *Pinus contorta* and *P. sylvestris*.

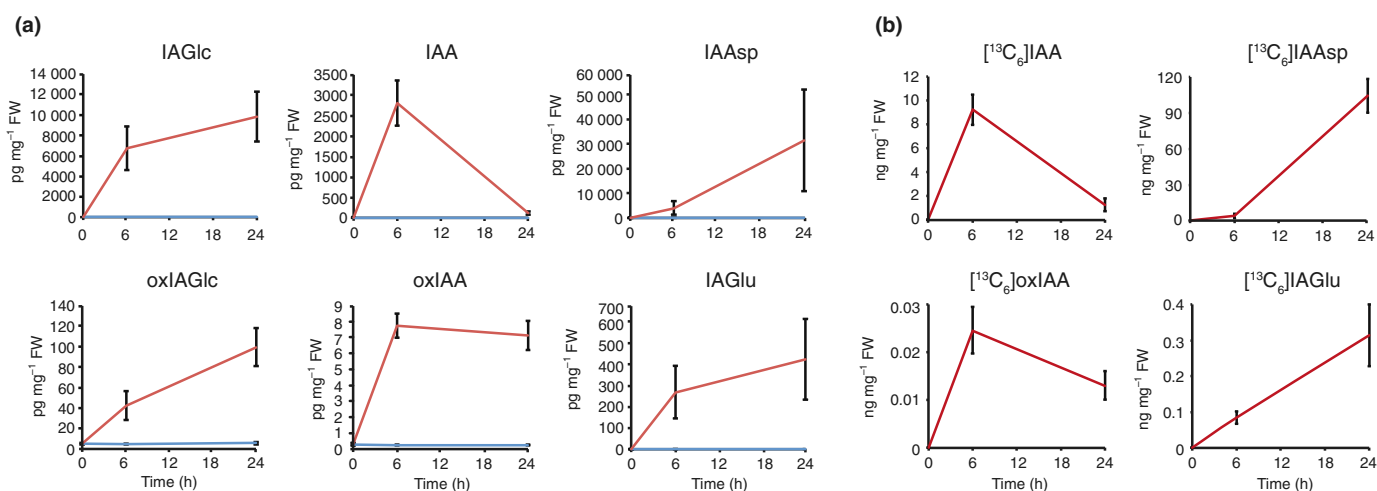


**Fig. 2** Concentrations of IAA metabolites in *Picea abies* roots after feeding with unlabelled or labelled IAA. (a) Two-week-old spruce seedlings were incubated with (red line) or without (blue line) 10  $\mu$ M unlabelled IAA and the concentrations of IAA and IAA metabolites oxIAA, oxIAGlc, IAGlc, IAAsp and IAGlu were quantified in roots after different incubation times. The concentrations of all metabolites are in picograms per milligram fresh weight (FW). (b) Two-week-old spruce seedlings were incubated with 10  $\mu$ M [ $^{13}\text{C}_6$ ]-IAA and the concentrations of [ $^{13}\text{C}_6$ ]-oxIAA, [ $^{13}\text{C}_6$ ]-IAAsp and [ $^{13}\text{C}_6$ ]-IAGlu were quantified in roots after different incubation times. The concentrations of all metabolites are in nanograms per milligram FW. Error bars indicate  $\pm$  SD ( $n = 4$  or  $n = 5$ , respectively). See Supporting Information Fig. S3 for IAA profiling after feeding with unlabelled IAA from *Pinus contorta* and *P. sylvestris*.

Together, these results indicate that the irreversible conjugation to form IAAsp and IAGlu was rapidly activated by increased free IAA concentrations in conifer seedlings.

To study the rates of IAA degradation in spruce roots, we then performed a feeding experiment in which [ $^{13}\text{C}_6$ ]-IAA was applied to whole seedlings and the degradation of IAA was measured by quantification of labelled IAA metabolites in roots. Feeding labelled IAA resulted in the formation of mainly [ $^{13}\text{C}_6$ ]-IAAsp, low concentrations of [ $^{13}\text{C}_6$ ]-IAGlu and almost no [ $^{13}\text{C}_6$ ]-oxIAA after 6 or 24 h (Fig. 2b), in accordance with the results obtained with unlabelled IAA (Fig. 2a). These findings indicate that the high endogenous concentrations of IAAsp and IAGlu observed in spruce originated from *de novo* synthesis.

The spruce genome has several *GH3* genes that belong to Group II of the *GH3* family

Our metabolic data have highlighted the importance of irreversible conjugative pathways for the regulation of IAA homeostasis in conifers. Auxin-conjugating enzymes of Group II of the GH3 family mediate the formation of IAAsp and IAGlu in Arabidopsis and this mechanism seems to be highly conserved over the entire plant kingdom (Staswick *et al.*, 2005; Terol *et al.*, 2006; Reddy *et al.*, 2006; Ludwig-Müller *et al.*, 2009; Ludwig-Müller, 2011). To identify the genes responsible for the conjugation of IAA with amino acids in conifers, we analysed the GH3 family of IAA-amido synthases and used *P. abies* as model species

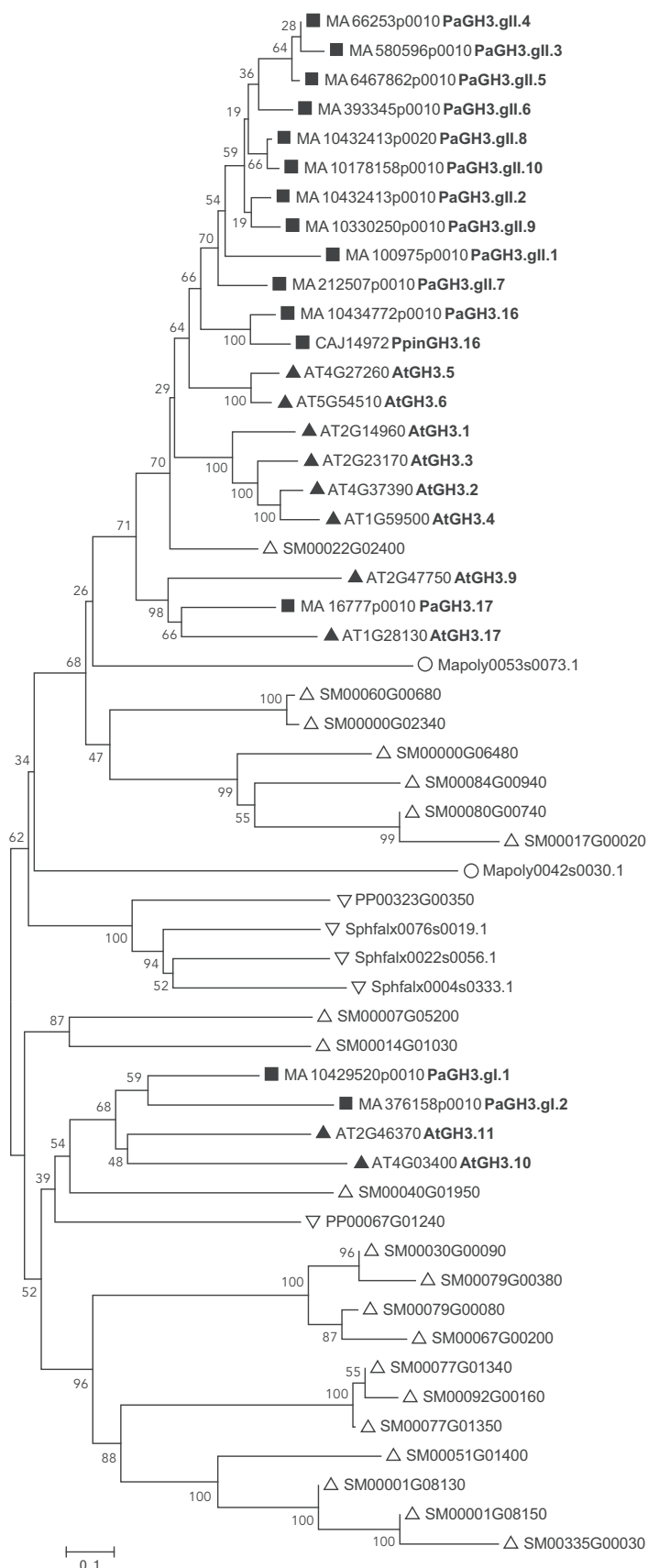
due to the availability of genomic resources (Nystedt *et al.*, 2013). Putative *GH3* genes of *P. abies* were retrieved using the gene family information present in PlantGenIE and were further examined by manual curation of protein motif scans using PFAM (<http://pfam.xfam.org/>; El-Gebali *et al.*, 2019) for the GH3 motif (PFAM id: 03321; GH3 auxin-responsive promoter). This allows the identification of 14 *P. abies* genes (hereafter referred to as *PaGH3* genes) encoding full-length or partial GH3 proteins (Fig. 3). We named these genes according to their putative orthologues in Arabidopsis, as explained below. Only five *PaGH3* genes encode full-length proteins (PaGH3.17, PaGH3.16, PaGH3.gII.1, PaGH3.gII.8 and PaGH3.gII.9), while the remaining nine are partial genes, lacking a portion in either the amino-, the carboxy- or both terminal regions. Three conserved sequence motifs involved in ATP/AMP binding that are characteristic of the acyl-adenylate/thioester-forming enzyme superfamily were previously identified and shown to be also conserved in the GH3 family (Staswick *et al.*, 2002; Terol *et al.*, 2006). Multiple alignment with the available deduced amino acid GH3 sequences from *P. abies* and Arabidopsis showed that all five full-length proteins, together with the partial protein sequence from PaGH3.gII.7, contain the three motifs, the partial proteins harbouring either the N-terminal (PaGH3.gII.4 and PaGH3.gI.2) or the C-terminal (PaGH3.gII.2 and PaGH3.gI.1) carry motifs 1 or 3, respectively (Fig. S5). The partial protein sequences from PaGH3gII.3, PaGH3gII.5, PaGH3gII.6 and PaGH3gII.10 did not contain any of the three motifs and only show conserved residues at the very C-terminal region (Fig. S5). The conservation of the three motifs in full-length PaGH3 proteins suggests that they might be able to bind ATP/AMP. The *GH3* gene family in Arabidopsis is composed of three subgroups, based on sequence similarities and protein function (Hagen *et al.*, 2002; Terol *et al.*, 2006; Okrent & Wildermuth, 2011). Among members of Group I, GH3.11 displays jasmonic acid (JA)-amino synthetase activity (Staswick *et al.*, 2002, 2005; Terol *et al.*, 2006; Gutierrez *et al.*, 2012). However, sequence homology among Group I members does not rule out the possibility of a preference for an additional substrate(s) because the two characterised *Physcomitrella patens* GH3s falling within this group can conjugate both IAA and JA to amino acids (Bierfreund *et al.*, 2004; Ludwig-Müller *et al.*, 2009). Group II contains proteins that conjugate IAA and/or JA and salicylic acid (SA) to amino acids (Staswick *et al.*, 2002, 2005; Terol *et al.*, 2006; Gutierrez *et al.*, 2012; Westfall *et al.*, 2016). Members of Group III were only found in Arabidopsis and some other Eurosids (Terol *et al.*, 2006). To determine the evolutionary position of the spruce *GH3* family members, a phylogenetic analysis was constructed including Arabidopsis Group I and II GH3s, predicted GH3-like protein sequences from early land plants such as liverwort (*Marchantia polymorpha*), mosses (*P. patens* and *Sphagnum fallax*) and a lycophyte (*Selaginella moellendorffii*) (Fig. 3). Two out of 14 PaGH3s were found in Group I and thus were named PaGH3.gI.1 and PaGH3.gI.2 (Fig. 3). Twelve out of 14 PaGH3s fell within Group II (Fig. 3). Two of these, PaGH3.17 and PaGH3.16, specifically clustered with AtGH3.17 and PpinGH3.16, respectively, and were named according to their potential orthologues in Arabidopsis or

*P. pinaster* (Fig. 3). The remaining PaGH3s of Group II clustered together in a subgroup closely related to AtGH3.5 and AtGH3.6 and therefore we gave them the generic name PaGH3.gII (from 1 to 10) (Fig. 3). The split between the two main groups (I and II) occurred very early as moss proteins were present in both main clusters, confirming previous results (Terol *et al.*, 2006; Fig. 3). Most of the GH3-like sequences from *Selaginella* form two specific subclusters within Group I and II, respectively, and only two lycophyte proteins are closely related to seed plant main clusters (Fig. 3). Within Group II, moss proteins also form a specific sub-cluster and liverworts are closely related to the lycophyte subgroup. Based on this evidence, the most likely explanation is for the split between the two main groups pre-dating even the most basal land plants and the vascular nonseed plants. Angiosperms and conifer GH3 proteins have evolved from few copies from that common ancestor, whereas the other land plants (bryophytes and lycophyte) have experienced a separate extension. In seed plants, the topology of the tree reflects the separation of gymnosperms and angiosperms, suggesting that there was a rapid evolution of the GH3 family even before the monocot–dicot split, as indicated by the strict subclustering between angiosperms and conifer GH3 proteins (Fig. 3). To assess the relationships of the PaGH3 proteins with other seed plants, an additional phylogenetic analysis was carried out including sequences from another conifer (*P. taeda*), woody dicots (*P. trichocarpa* and *M. domestica*) and a monocot (*O. sativa*) (Fig. S6). All the PaGH3s have a corresponding orthologous counterpart in pine and their sequences subcluster together. Sequences split into different subclusters with a clear-cut separation between gymnosperms and angiosperms. Nonetheless, few rice sequences were found to cluster with pine GH3s, indicating that these sequences might be distantly related to Arabidopsis GH3s, as previously reported (Terol *et al.*, 2006).

#### A subset of *PaGH3* genes is auxin-inducible and catalyses the conjugation of IAA to Asp and Glu

To determine whether the accumulation of irreversible amide-linked conjugates could be related to modifications of the expression of auxin conjugation genes, the response of *PaGH3* genes to exogenous auxin treatment was analysed using qRT-PCR. Spruce seedlings were treated with or without 10 µM IAA for 6 h and gene expression was studied in root tissues. Two partial *PaGH3* genes (*PaGH3.gII.6* and *PaGH3.gII.10*) were excluded from our analysis as the partial nucleotide sequence of *PaGH3.gII.10* was not distinguishable from the full-length sequence of *PaGH3.gII.8* and transcripts from *PaGH3.gII.6* were not detected under our experimental conditions. After auxin treatment, the relative transcript level of nine *PaGH3* genes (*PaGH3.gII.9*, *PaGH3.gII.5*, *PaGH3.gII.3*, *PaGH3.16*, *PaGH3.gII.8*, *PaGH3.gII.2*, *PaGH3.gII.4*, *PaGH3.gII.7* and *PaGH3.17*) was increased, while that of *PaGH3.gII.1*, *PaGH3.gI.1* and *PaGH3.gI.2* was either reduced or not affected (Fig. 4). The finding that the two *PaGH3* genes from Group I were not induced by auxin is consistent with previous studies which concluded that *AtGH3.10* and *AtGH3.11* were not auxin-inducible genes (Hagen *et al.*, 2002; Winter *et al.*,

**Fig. 3** Phylogenetic relationships of GH3 proteins between *Picea abies* and basal land plants. Predicted protein sequences (both full-length and partial) from *P. abies* (MA), *Pinus pinaster* (Ppin), *Arabidopsis thaliana* (AT), *Selaginella moellendorffii* (SM), *Physcomitrella patens* (PP), *Sphagnum fallax* (Sphfalx) and *Marchantia polymorpha* (Mapoly) were aligned using the program MUSCLE. The phylogenetic tree was constructed using MEGA6 and the neighbor-joining method with predicted GH3 proteins. Bootstrap support is indicated at each node. Closed triangle, angiosperms; closed square, gymnosperms; upward open triangle, lycophytes; downward open triangle, mosses; open circle, liverworts. Scale bar indicates number of changes per site.



Group II

Group I

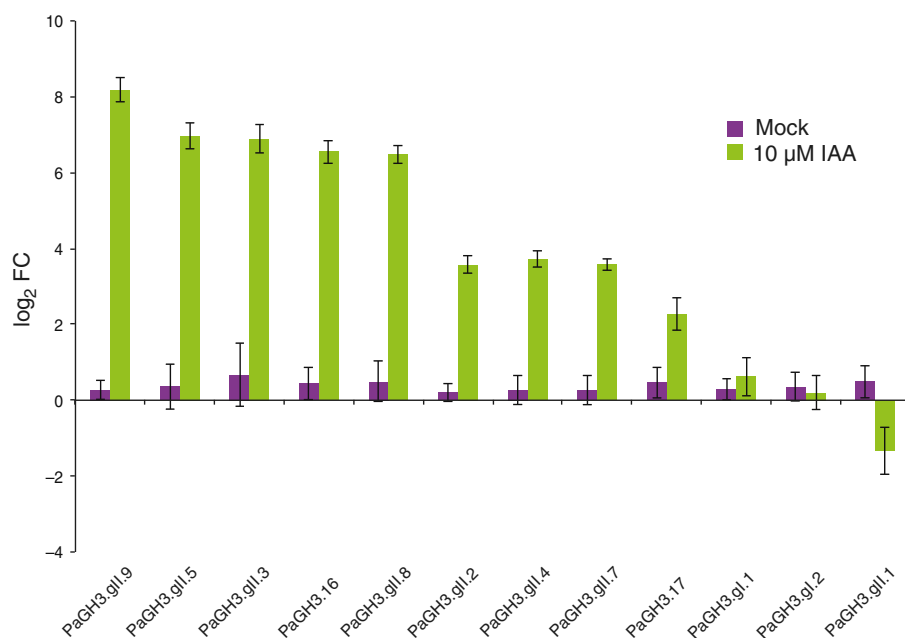


**Fig. 4** Expression profile of *PaGH3* genes after treatment with auxin. qRT-PCR analysis was performed using cDNA from roots of 2-wk-old spruce seedlings treated with or without 10 μM IAA for 6 h. Fold change (FC) was calculated via the comparative cycle threshold (Ct) method and values were normalised based on expression of the *Paelf4A* gene. Expression of *PaGH3.gII.6* and *PaGH3.gII.10* genes was not detected in our experimental conditions. Error bars represent ± SD from three biological replicates.

2007; Okrent & Wildermuth, 2011). This corroborates the observed orthologous relationship of these *Arabidopsis* and spruce *GH3* genes. Intrigued by the results of our phylogenetic and expression analyses, we cloned four of the auxin-inducible *PaGH3* genes and tested their IAA-conjugation activity. *PaGH3* proteins were expressed in *E. coli* individually, and the expression of recombinant fusion proteins was confirmed by Western blot analysis (Fig. S7). Cultures of *PaGH3.16*-, *PaGH3.17*-, *PaGH3.gII.8*- and *PaGH3.gII.9*-expressing bacteria were tested in a reaction with or without 0.1 mM IAA in combination with GH3 cofactor mixture, as these conditions were previously optimised for *AtGH3*-mediated IAA<sub>Asp</sub> and IAGlu production (Brunoni *et al.*, 2019). Fig. 5 shows that, while the reaction mediated by *PaGH3.16* led to the accumulation of very low amounts of IAA<sub>Asp</sub> and IAGlu, the reaction mediated by the other *PaGH3*s tested led to the accumulation of very high concentrations of IAA<sub>Asp</sub> and/or IAGlu. *PaGH3.17* preferred Glu over Asp, similarly to its *Arabidopsis* orthologue GH3.17 (Staswick *et al.*, 2005; Brunoni *et al.*, 2019) (Fig. 5). Interestingly, the reaction mediated by *PaGH3.gII.8* yielded the accumulation of both amide-linked conjugates but IAA was conjugated more efficiently with Asp than Glu, as IAA<sub>Asp</sub> levels were much higher than IAGlu (Fig. 5). Although to a minor extent compared to *PaGH3.gII.8*, bacterial cultures expressing *PaGH3.gII.9* accumulated higher concentrations of IAA<sub>Asp</sub> than IAGlu, suggesting that this enzyme also prefers Asp over Glu (Fig. 5). Accumulation of IAA<sub>Asp</sub> and IAGlu was always below the limit of detection in all mock samples (Fig. 5). Our results demonstrate that at least three Norway spruce GH3 proteins, *PaGH3.17*, *PaGH3.gII.8* and *PaGH3.gII.9*, are able to conjugate IAA with Asp and/or Glu, supporting the finding that these GH3 proteins are responsible for irreversible amide-linked conjugation, thus maintaining IAA homeostasis in spruce.

*Pa2OGD* members of the nearest group to DAOs do not catalyse the oxidation of IAA to oxIAA

The oxidation of IAA to oxIAA is one of the major catabolic pathways to inactivate auxin in higher plants, early land plants and algae (Östin *et al.*, 1998; Peer *et al.*, 2013; Pěncík *et al.*, 2013; Drábková *et al.*, 2015; Žizková *et al.*, 2017). Recent findings have demonstrated that the DAO enzymes catalyse conversion of IAA to oxIAA (Zhao *et al.*, 2013; Porco *et al.*, 2016; Zhang *et al.*, 2016). These proteins share a high similarity to each other and very low similarity to the other 2OGD family members, making them a novel subfamily (Zhang *et al.*, 2016). Surprisingly, our metabolic data revealed that the irreversible oxidative pathway plays a marginal role in maintaining IAA homeostasis in conifers. To verify if the formation of oxIAA in Norway spruce could be ascribed to any DAO-like enzyme, we first checked if DAO-like genes are conserved in spruce by blasting the *AtDAO1* protein sequence against the ConGenIE.org (Conifer Genome Integrative Explorer) database. The resulting spruce protein sequences with high confidence prediction were further examined by manual curation of protein motif scans using PFAM for the DIOX\_N motif (PFAM id: 14226) and the 2OG-FeII\_Oxy (PFAM id: 03171). Only putative spruce 2OGDs harbouring these two motifs were included in further analysis because only the presence of these two motifs at the N- and C-terminus, respectively, would suggest their involvement in specialised metabolism of phytochemicals, rather than nucleotide and protein modification (Kawai *et al.*, 2014). A similar approach was undertaken to retrieve putative 2OGDs from *P. taeda*, basal land plants and chlorophytes. To investigate the evolutionary relationships of these selected putative 2OGD family members from nonflowering plants and chlorophytes to angiosperm DAOs, a comprehensive phylogenetic analysis was undertaken (Fig. S8). Our analysis shows that the DAO clade includes only

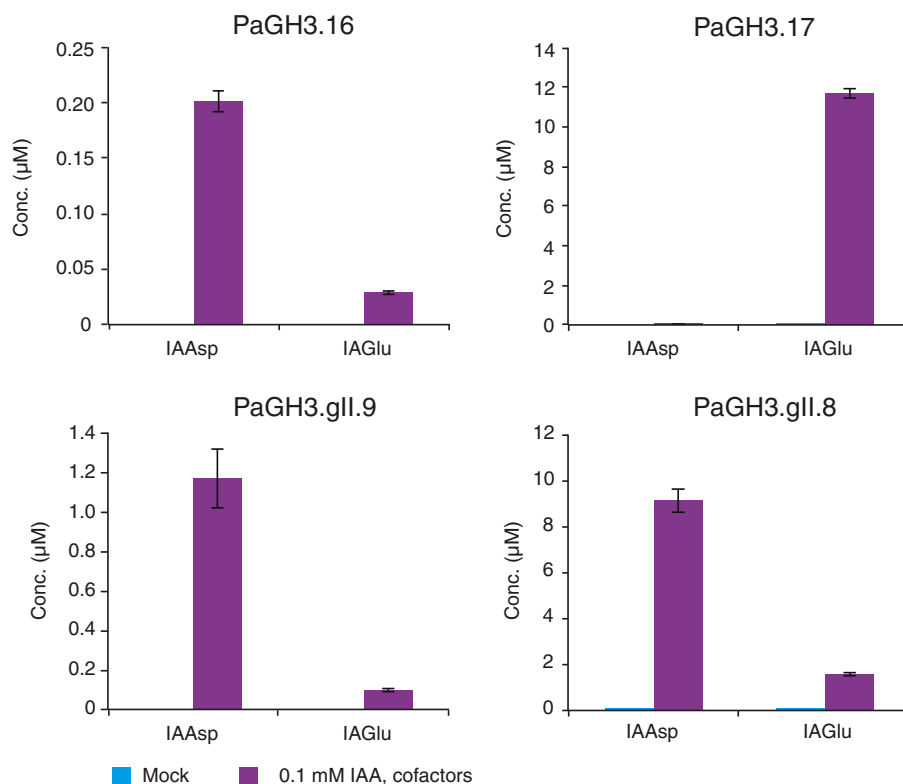


**Fig. 5** IAA conjugation activity of recombinant PaGH3.16, PaGH3.17, PaGH3.gll.8 or PaGH3.gll.9 proteins. The evaluation of enzyme reactions for IAAsp and IAGlu formation was performed using PaGH3.16-, PaGH3.17-, PaGH3.gll.8- or PaGH3.gll.9-expressing bacterial cultures. All the bacterial cultures were incubated with 0.1 mM IAA and with cofactor mixture (1 mM glutamic acid, 1 mM aspartic acid, 3 mM ATP and 3 mM MgCl<sub>2</sub>) for 6 h at 20°C and only supernatant fractions were analysed. Bacterial cultures without IAA and cofactor mixture were used as mock samples. Values are mean  $\pm$  SD ( $n = 3$ ).

sequences retrieved from angiosperms, but no 2OGDs from non-flowering plants or chlorophytes, confirming previous results (Kawai *et al.*, 2014). Nonetheless, a distinct group of putative 2OGDs from spruce and pine was found to be the nearest neighbour to the DAO clade (Fig. S8). This conifer group splits into two subgroups and, among the eight putative spruce 2OGDs falling within this group, three clustered in the first subgroup, while the remaining five were found in the second subgroup (Fig. S8). We named these eight spruce 2OGD genes (hereafter referred to as *Pa2OGD* genes) from 1 to 8 according to their proximity to the DAO clade (Fig. S8). To test the ability to oxidise IAA of *Pa2OGDs* that are close to the DAO clade, four spruce 2OGD genes (*Pa2OGD.1* and *Pa2OGD.2* from the first subgroup, and *Pa2OGD.6* and *Pa2OGD.8* from the second subgroup) were cloned and expressed in *E. coli* individually, and the expression of recombinant fusion proteins was confirmed by Western blot analysis (Fig. S9a). Cultures of *Pa2OGD.1*-, *Pa2OGD.2*-, *Pa2OGD.6*- and *Pa2OGD.8*-expressing bacteria were tested in a reaction with or without 10  $\mu$ M IAA in combination with DAO cofactor mixture, as these conditions were previously optimised for AtDAO1-mediated oxIAA production (Brunoni *et al.*, 2019). In stark contrast to IAA-treated AtDAO1 samples, low concentrations of oxIAA were detected in all the *Pa2OGD* samples and no differences in oxIAA concentrations were observed among them, any green fluorescent protein (GFP) samples nor mock AtDAO1 sample (Fig. S9b). This indicates that the detected oxIAA in *Pa2OGD* samples originated from nonenzymatic oxidation of IAA that occurs in the culture media, as previously reported (Brunoni *et al.*, 2019). Our results demonstrate that none of the tested spruce 2OGDs are able to oxidise

IAA, corroborating the observed phylogenetic separation between the *Pa2OGDs* and the DAO clade. This indicates that the oxidative catabolism of IAA mediated by DAOs is likely to be restricted to angiosperms.

## Discussion

Maintaining appropriate auxin concentrations is critical for regulating all aspects of plant growth and development. Regulation of auxin homeostasis via conjugation and catabolism has been suggested to be a significant contributor to this process. IAA conjugation and degradation pathways and the key components of their machineries have been identified and well-characterised in *Arabidopsis* by incorporating results obtained from gene expression and functionality studies and metabolic analyses. The formation of oxIAA was shown to be a major pathway for IAA degradation, acting redundantly and cooperatively with reversible and irreversible IAA conjugation to maintain steady-state auxin concentrations in *Arabidopsis*. A proposed model for catabolic regulation of IAA in *Arabidopsis* reveals that the DAO-mediated oxidation pathway finely tunes basal auxin concentrations under normal growth conditions while the GH3-dependent conjugation pathway responds to both developmental and environmental stimuli (Park *et al.*, 2007; Mellor *et al.*, 2016; Porco *et al.*, 2016).

Our understanding of the physiological mechanisms modulating IAA content in gymnosperms is much less well understood. Nonetheless, it seems that auxin degradation and conjugation are conserved mechanisms also in gymnosperms, but the contribution of these processes in maintaining IAA homeostasis has not yet been elucidated. Comparative studies of gymnosperms and

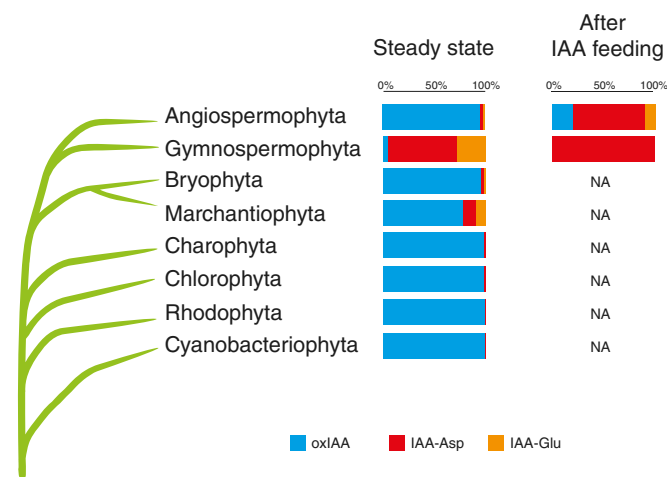


**Fig. 6** Schematic illustration of the most well-studied IAA inactivation pathways in land plants, algae and cyanobacteria. The proportion of oxIAA, IAAsp and IAGlu in the total IAA catabolite pool under steady-state conditions for Cyanobacteria, Rhodophyta, Chlorophyta, Charophyta (Žižková *et al.*, 2017), Marchantiophyta, Bryophyta (Drábková *et al.*, 2015), Gymnospermophyta (this study) and Angiospermophyta (Porco *et al.*, 2016) is reported. The proportion of IAA irreversible catabolites after feeding with labelled IAA for angiosperms (Porco *et al.*, 2016) and gymnosperms (this study) is reported. NA, not available.

angiosperms are the key to gain a better understanding of the genetic regulation of the mechanisms responsible for the diversification of IAA action in seed plants. Within gymnosperms, conifers represent the major division, comprising two-thirds of the extant lineage and they have huge ecological and economic importance. The recent release of genome drafts for spruces and pines have opened new possibilities for studying regulatory gene functions in conifers. Here, we have studied the contribution of regulatory processes to maintain optimal concentrations of IAA in seedlings from three different conifer species (*P. abies*, *P. sylvestris* and *P. contorta*), and investigated the conservation of key molecular mechanisms involved in the degradation of IAA in Norway spruce. The long generation time of conifers makes it difficult to perform studies of gene function, so we used young seedlings as an experimental system to study IAA inactivation pathways in conifers. We investigated the shift of IAA metabolite content under steady-state conditions and after exogenously applied IAA. Interestingly, we observed that, among the primary IAA catabolites, oxIAA accumulated at very low concentrations in all the tissues analysed from conifer seedlings under steady-state growth conditions (Figs 1, S2). By contrast, we observed that the other two primary catabolites, the amide conjugates IAAsp and IAGlu, contributed more than oxIAA to IAA catabolism in conifers under steady-state conditions. Perturbation of IAA homeostasis by feeding with exogenous IAA confirmed the observed metabolic pattern, as conifer seedlings accumulated these two irreversible amide-linked conjugates in much higher concentrations compared to oxIAA (Figs 2a, S3). A feeding experiment using labelled IAA revealed that IAAsp was the primary IAA catabolite originating from *de novo* synthesis, highlighting the production of IAAsp as the favourite route for IAA degradation in spruce (Fig. 2b). In Arabidopsis seedlings,

the glucosylester oxIAGlc is the most abundant IAA catabolite (Kai *et al.*, 2007; Porco *et al.*, 2016), and it is probably synthesised via glucosylation of oxIAA and not oxidation of IAGlc, suggesting that concentrations of oxIAGlc could mirror those of oxIAA. In conifer seedlings, we found that, similarly to oxIAA, oxIAGlc was also detected at very low concentration, confirming that the oxidation pathway plays a minor role in modulating IAA content in conifer seedlings compared to Arabidopsis (Figs 1, S2). In conifers, glucose conjugation to IAA also contributed to the inactivation of IAA under steady-state conditions or after exogenous treatment with IAA (Figs 1, 2a, S2, S3). The formation of IAGlc is a well-known mechanism for IAA inactivation and this ester-linked conjugate is considered as a reversible storage form, the content of which depends on the conjugation/hydrolysis rates (Jackson *et al.*, 2001). Together, these findings indicated that, on the one hand, oxIAA formation contributed less to the maintenance of steady-state IAA concentrations in conifer seedlings, both under steady-state growth conditions and after treatment with exogenous IAA, and, on the other hand, the conversion of IAA to IAAsp and IAGlu appeared to be a major catabolic pathway, acting at a constitutive level and after IAA homeostasis perturbation in conifer seedlings. These findings do not preclude that these mechanisms could differentially contribute to reduce IAA content at other developmental stages or under different growth conditions and that conifers could possess other IAA inactivation pathway(s) that have not yet been identified.

The GH3 auxin-conjugating enzymes from Group II mediate the formation of IAAsp and IAGlu in Arabidopsis and this pathway seems to be highly conserved over the entire plant kingdom (Staswick *et al.*, 2005; Terol *et al.*, 2006; Reddy *et al.*, 2006; Ludwig-Müller *et al.*, 2009; Ludwig-Müller, 2011). We have therefore focused on the molecular identification of spruce GH3 homologues that could be involved in the formation of the amide-linked conjugates IAAsp and IAGlu. Phylogenetic analysis showed a homology clustering consistent with the functional classification of the Arabidopsis proteins, as the PaGH3 sequences grouped into the two main clusters, corresponding to Arabidopsis functional groups I (JA adenylation) and II (IAA adenylation) as shown in Fig. 3. A comparative phylogenetic analysis including GH3 sequences from genomes of relevant taxonomic lineages showed a strict subclustering between angiosperms and conifer GH3 proteins, suggesting that the evolution of the family predated the separation of gymnosperms and angiosperms (Figs 3, S6). In Arabidopsis, the expression of several Arabidopsis GH3 genes of Group II is induced by exogenously applied auxin, while *AtGH3.9*, *AtGH3.17* and the *AtGH3s* of Group I show little or no induction by auxin (Hagen *et al.*, 2002; Winter *et al.*, 2007; Okrent & Wildermuth, 2011; Di Mambro *et al.*, 2017). *PpinGH3.16*, the only other Group II GH3 homologue from conifers studied so far, was also specifically up-regulated after auxin treatment (Reddy *et al.*, 2006). Plants have developed a feedback mechanism to control the concentrations of active auxin through modulation of GH3 gene expression by auxin itself (Staswick *et al.*, 2005). Expression analysis of *PaGH3* genes revealed that nine *PaGH3s* of Group II were highly up-regulated after treatment with IAA, while the other *PaGH3* of Group II (*PaGH3.gII.1*), and *PaGH3s* of Group I were either down-

regulated or not induced by auxin (Fig. 4). The differential response to auxin among the *PaGH3* genes mirrors the phylogenetic clustering of the corresponding enzymes (Fig. 3). Most of Arabidopsis Group II enzymes are demonstrated to be active on IAA and each GH3 enzyme has a broad specificity for amino acids and could synthesise several types of IAA–amino acid conjugates (Staswick *et al.*, 2005). Nonetheless, evaluation of GH3 enzyme activity with different amino acids *in vitro* and GH3 multiple mutant analyses revealed that IAA<sub>Asp</sub> is a major conjugate formed by AtGH3.1–6 and that IAGlu formation is mediated by AtGH3.17 (Staswick *et al.*, 2005; Porco *et al.*, 2016). Heterologously expressed AtGH3.6 and AtGH3.17 also efficiently conjugate IAA with Asp and/or Glu in a bacterial assay (Brunoni *et al.*, 2019). We therefore investigated possible IAA-conjugating activity with Asp and Glu for four of the auxin-inducible PaGH3-recombinant proteins by performing the enzymatic assay directly in bacterial cultures (Fig. 5). Among them, PaGH3.17 enzyme conjugated IAA mainly to Glu, suggesting that PaGH3.17 and AtGH3.17 could be functionally equivalent. By contrast, PaGH3.16, PaGH3.gII.9 and PaGH3.gII.8 appeared to favour Asp over Glu, as IAA<sub>Asp</sub> accumulated more than IAGlu. Here, we have found that these GH3 proteins are responsible for irreversible amide-linked conjugates and, thus, could function redundantly in reducing IAA concentrations in spruce.

IAA oxidation has long been the most elusive step in IAA metabolism. Both soluble and membrane-associated cell fractions were observed to oxidise auxin (reviewed by Zhang & Peer, 2017). The enzymes that catalyse IAA oxidation were only recently identified in angiosperms and extensively characterised in Arabidopsis. These proteins share high similarity to each other and very low similarity to the other 2OGD family members, making them a novel subfamily. In addition, AtDAO1 was shown to be a soluble protein with cytosolic localisation and not associated with membranes (Porco *et al.*, 2016; Zhang *et al.*, 2016). In an attempt to verify if the formation of oxIAA in spruce could be ascribed to any DAO-like enzymes, a comparative phylogenetic analysis was undertaken using putative 2OGD proteins from spruce and landmark genomes. No 2OGDs from spruce, any other nonflowering plants or chlorophytes were found to cluster within the DAO clade (Fig S8), confirming previous findings reported by Kawai *et al.* (2014). Enzymatic assays with recombinant Pa2OGDs revealed that not even the Pa2OGD proteins that are nearest neighbours to the DAO clade are able to oxidise IAA (Fig. S9), confirming that, in stark contrast to angiosperms, the oxidative catabolism of IAA is not mediated by DAO-like proteins in spruce. We cannot rule out that some as yet unidentified membrane-associated proteins could be responsible for IAA oxidation in nonflowering plants and algae.

The available evidence supports the perspective that the pathways for IAA oxidation and conjugation are the predominant IAA homeostatic pathways operating in all land plants and algae. While both charophytes and liverworts use a more primitive regulatory strategy to deal with excess IAA, which is based on the control of the balance between the rates of IAA biosynthesis and IAA degradation, more sophisticated machineries have later evolved (Sztein *et al.*, 1999; Cooke *et al.*, 2002). As a result, IAA

conjugation and conjugate hydrolysis reactions have developed and started to play a more important role in the regulation of auxin homeostasis in all the other land plants. It is believed that this metabolic implementation allows plants to achieve a more precise spatial and temporal control of IAA accumulation (Sztein *et al.*, 1999; Cooke *et al.*, 2002). Since then, new methods for more precise and sensitive IAA metabolite profiling have been developed and used to retrieve data from several species ranging from cyanobacteria and algae to several bryophytes (Drábková *et al.*, 2015; Žižková *et al.*, 2017). The bulk of new data available have highlighted that oxidation is a major pathway for IAA degradation in algae, in basal land plants and in angiosperms, while it seems to be of minor importance in conifers (Fig. 6). Arabidopsis has developed an IAA homeostatic response based on a slow oxidative mechanism that constitutively modulates the optimal auxin concentrations and a fast conjugative and inducible pathway that reduces IAA from the active auxin pool upon stress or developmental cues (Fig. 6). This metabolic pattern seems to arise from pre-existing elements of the IAA inactivation machinery already operating in green algae and mosses and contributing to regulate concentrations of active auxin similarly to Arabidopsis. First, IAA catabolism via oxidation was found to be a more relevant homeostatic mechanism than the conjugative pathway in cyanobacteria, algae and the most basal land plants (Fig. 6) (Drábková *et al.*, 2015; Žižková *et al.*, 2017). Second, results from feeding several algae species with IAA demonstrated that the IAA conjugative pathway is rapidly activated, as IAA<sub>Asp</sub> and IAGlc were the two major products. Interestingly, the metabolism of exogenously labelled IAA in these selected algal species led to the detection of several more unidentified metabolites, indicating the existence of other unknown IAA metabolic pathway(s) in green algae (Žižková *et al.*, 2017). By contrast, conifers seem to prefer to rely mainly on a conjugative mechanism for fine-tuning basal IAA concentrations under steady-state conditions and that can be rapidly activated in response to exogenously applied IAA (Fig. 6). Together, our findings suggest that the strategy adopted by conifers to maintain homeostatic levels of endogenous IAA differs from all other land plants and algae studied so far. Further studies in other gymnosperm taxa and at other developmental stages would add further tiles to confirm that this diversification of IAA action is conserved in the lineage of gymnosperms.

## Acknowledgements









This research was supported by grants from the Swedish research councils FORMAS, VR, Kempestiftelserna, and the Knut and Alice Wallenberg Foundation (to KL and CB). We thank Dr Mikael Lindberg of the Protein Expression Platform (PEP, Umeå, Sweden) for cloning the Pa2OGD genes, Dr Nicolas Delhomme for helpful discussions and the Swedish Metabolomics Center (SMC, Umeå, Sweden) for access to instrumentation.

## Author contributions

FB, SC, RC-S, MS, KL and CB conceived and designed the experiments. FB, SC, RC-S, JS and MK performed all the

experiments. FB and SC wrote the manuscript with input from all authors. All authors read and approved the final article for publication.

## ORCID

Catherine Bellini  <https://orcid.org/0000-0003-2985-6649>  
 Federica Brunoni  <https://orcid.org/0000-0003-1497-9419>  
 Rubén Casanova-Sáez  <https://orcid.org/0000-0001-5683-7051>  
 Silvio Collani  <https://orcid.org/0000-0002-9603-0882>  
 Michal Karady  <https://orcid.org/0000-0002-5603-706X>  
 Karin Ljung  <https://orcid.org/0000-0003-2901-189X>  
 Markus Schmid  <https://orcid.org/0000-0002-0068-2967>  
 Jan Šimura  <https://orcid.org/0000-0002-1567-2278>

## References

- Bierfreund NM, Tintelnot S, Reski R, Decker EL. 2004. Loss of GH3 function does not affect phytochrome-mediated development in a moss *Physcomitrella patens*. *Plant Cell Reports* 21: 1143–1152.
- Biról I, Raymond A, Jackman SD, Pleasance S, Coope R, Taylor GA, Saint YMM, Keeling CI, Brand D, Vandervalk BP *et al.* 2013. Assembling the 20 Gb white spruce (*Picea glauca*) genome from whole-genome shotgun sequencing data. *Bioinformatics* 29: 1492–1497.
- Brunoni F, Collani S, Šimura J, Schmid M, Bellini C, Ljung K. 2019. A bacterial assay for rapid screening of IAA catabolic enzymes. *Plant Methods* 15: 126.
- Cooke TJ, Poli DB, Szein AE, Cohen JD. 2002. Evolutionary patterns in auxin action. *Plant Molecular Biology* 49: 319–338.
- Di Mambro R, De Ruvo M, Pacifici E, Salvi E, Sozzani R, Benfey PN, Busch W, Novak O, Ljung K, Di Paola L *et al.* 2017. Auxin minimum triggers the developmental switch from cell division to cell differentiation in the Arabidopsis root. *Proceedings of the National Academy of Sciences, USA* 114: E7641–E7649.
- Drábková LZ, Dobrev PI, Motyka V. 2015. Phytohormone profiling across the bryophytes. *PLoS ONE* 10: 1–19.
- Edgar RC. 2004. MUSCLE: multiple sequence alignment with high accuracy and high throughput. *Nucleic Acids Research* 32: 1792–1797.
- El-Gebali S, Mistry J, Bateman A, Eddy SR, Luciani A, Potter SC, Qureshi M, Richardson LJ, Salazar GA, Smart A *et al.* 2019. The Pfam protein families database in 2019. *Nucleic Acids Research* 47: D427–D432.
- Goodstein DM, Shu S, Howson R, Neupane R, Hayes RD, Fazo J, Mitros T, Dirks W, Hellsten U, Putnam N *et al.* 2012. Phytozome: a comparative platform for green plant genomics. *Nucleic Acids Research* 40: 1178–1186.
- Gutierrez L, Mongelard G, Floková K, Pácurar DI, Novák O, Staswick PE, Kowalczyk M, Pácurar M, Demailly H, Geiss G *et al.* 2012. Auxin controls arabidopsis adventitious root initiation by regulating jasmonic acid homeostasis. *Plant Cell* 24: 2515–2527.
- Hagen G, Guilfoyle T, Okrent RA, Wildermuth MC. 2002. Evolutionary history of the GH3 family of acyl adenylases in rosids. *Plant Molecular Biology* 49: 489–505.
- Jackson RG, Lim EK, Li Y, Kowalczyk M, Sandberg G, Hogget J, Ashford DA, Bowles DJ. 2001. Identification and biochemical characterization of an Arabidopsis indole-3-acetic acid glucosyltransferase. *Journal of Biological Chemistry* 276: 4350–4356.
- Kai K, Horita J, Wakasa K, Miyagawa H. 2007. Three oxidative metabolites of indole-3-acetic acid from *Arabidopsis thaliana*. *Phytochemistry* 68: 1651–1663.
- Kawai Y, Ono E, Mizutani M. 2014. Evolution and diversity of the 2-oxoglutarate-dependent dioxygenase superfamily in plants. *The Plant Journal* 78: 328–343.
- Kowalczyk M, Sandberg G. 2001. Quantitative analysis of indole-3-acetic acid metabolites in Arabidopsis. *Plant Physiology* 127: 1845–1853.
- Kramer EM, Ackelsberg EM. 2015. Auxin metabolism rates and implications for plant development. *Frontiers in Plant Science* 6: 1–8.
- LeClere S, Tellez R, Rampey RA, Matsuda SPT, Bartel B. 2002. Characterization of a family of IAA-amino acid conjugate hydrolases from Arabidopsis. *Journal of Biological Chemistry* 277: 20446–20452.
- Ljung K. 2013. Auxin metabolism and homeostasis during plant development. *Development* 140: 943–950.
- Ljung K, Östin A, Lioussanne L, Sandberg G. 2001. Developmental regulation of indole-3-acetic acid turnover in Scots pine seedlings. *Plant Physiology* 125: 464–475.
- Ludwig-Müller J. 2011. Auxin conjugates: their role for plant development and in the evolution of land plants. *Journal of Experimental Botany* 62: 1757–1773.
- Ludwig-Müller J, Jülke S, Bierfreund NM, Decker EL, Reski R. 2009. Moss (*Physcomitrella patens*) GH3 proteins act in auxin homeostasis. *New Phytologist* 181: 323–338.
- Mellor N, Band LR, Pěncík A, Novák O, Rashed A, Holman T, Wilson MH, Voß U, Bishopp A, King JR *et al.* 2016. Dynamic regulation of auxin oxidase and conjugating enzymes AtDAO1 and GH3 modulates auxin homeostasis. *Proceedings of the National Academy of Sciences, USA* 113: 11022–11027.
- Neale DB, Wegrzyn JL, Stevens KA, Zimin AV, Puiu D, Crepeau MW, Cardeno C, Koriabine M, Holtz-Morris AE, Liechty JD *et al.* 2014. Decoding the massive genome of loblolly pine using haploid DNA and novel assembly strategies. *Genome Biology* 15: 1–13.
- Normanly J. 2010. Approaching cellular and molecular resolution of auxin biosynthesis and metabolism. *Cold Spring Harbor Perspectives in Biology* 2: 1–18.
- Novák O, Hényková E, Sairanen I, Kowalczyk M, Pospíšil T, Ljung K. 2012. Tissue-specific profiling of the *Arabidopsis thaliana* auxin metabolome. *The Plant Journal* 72: 523–536.
- Nystedt B, Street NR, Wetterbom A, Zuccolo A, Lin YC, Scofield DG, Vezzi F, Delhomme N, Giacomello S, Alexeyenko A *et al.* 2013. The Norway spruce genome sequence and conifer genome evolution. *Nature* 497: 579–584.
- Okrent RA, Wildermuth MC. 2011. Evolutionary history of the GH3 family of acyl adenylases in rosids. *Plant Molecular Biology* 76: 489–505.
- Östin A, Kowalczyk M, Bhalerao RP, Sandberg G. 1998. Metabolism of indole-3-acetic acid in Arabidopsis. *Plant Physiology* 118: 285–296.
- Park JE, Park JY, Kim YS, Staswick PE, Jeon J, Yun J, Kim SY, Kim J, Lee YH, Park CM. 2007. GH3-mediated auxin homeostasis links growth regulation with stress adaptation response in Arabidopsis. *The Journal of Biological Chemistry* 282: 10036–10046.
- Peer WA, Cheng Y, Murphy AS. 2013. Evidence of oxidative attenuation of auxin signalling. *Journal of Experimental Botany* 64: 2629–2639.
- Pěncík A, Simonovik B, Petersson SV, Henykova E, Simon S, Greenham K, Zhang Y, Kowalczyk M, Estelle M, Zazimalova E *et al.* 2013. Regulation of auxin homeostasis and gradients in Arabidopsis roots through the formation of the indole-3-acetic acid catabolite 2-oxindole-3-acetic acid. *Plant Cell* 25: 3858–3870.
- Pfaff MW. 2001. A new mathematical model for relative quantification in real-time RT-PCR. *Nucleic Acids Research* 29: e45.
- Porco S, Pěncík A, Rashed A, Voß U, Casanova-Sáez R, Bishopp A, Golebiowska A, Bhosale R, Swarup R, Swarup K *et al.* 2016. Dioxygenase-encoding AtDAO1 gene controls IAA oxidation and homeostasis in Arabidopsis. *Proceedings of the National Academy of Sciences, USA* 113: 11016–11021.
- Reddy SM, Hitchin S, Melayah D, Pandey AK, Raffier C, Henderson J, Marmeisse R, Gay G. 2006. The auxin-inducible GH3 homologue Pp-GH3.16 is downregulated in *Pinus pinaster* root systems on ectomycorrhizal symbiosis establishment. *New Phytologist* 170: 391–400.
- Ruiz Rosquete M, Barbez E, Kleine-Vehn J. 2012. Cellular auxin homeostasis: gatekeeping is housekeeping. *Molecular Plant* 5: 772–786.
- Saitou N, Nei M. 1987. The neighbor-joining method: a new method for reconstructing phylogenetic trees. *Molecular Biology and Evolution* 4: 406–425.
- Schwarz R, Dayhoff M. 1979. Matrices for detecting distant relationships. In: Dayhoff M, ed. *Atlas of protein sequences*. Washington, DC, USA: National Biomedical Research Foundation, 353–358.
- Staswick PE, Serban B, Rowe M, Tiriyaki I, Maldonado MT, Maldonado MC, Suza W. 2005. Characterization of an Arabidopsis enzyme family that conjugates amino acids to indole-3-acetic acid. *Plant Cell* 17: 616–627.

- Staswick PE, Tiryaki I, Rowe ML. 2002. Jasmonate response locus *jar1* and several related *Arabidopsis* genes encode enzymes of the firefly luciferase superfamily that show activity on jasmonic, salicylic, and indole-3-acetic acids in an assay for adenylation. *Plant Cell* 14: 1405–1415.
- Szpanova AN, Alonso JM. 2016. Auxin catabolism unplugged: role of IAA oxidation in auxin homeostasis. *Proceedings of the National Academy of Sciences, USA* 113: 10742–10744.
- Sundell D, Mannapperuma C, Netotea S, Delhomme N, Lin YC, Sjödin A, Van de Peer Y, Jansson S, Hvidsten TR, Street NR. 2015. The plant genome integrative explorer resource: PantGenIE.org. *New Phytologist* 208: 1149–1156.
- Sztejn AE, Cohen JD, Garcia de la Fuente I, Cooke TJ. 1999. Auxin metabolism in mosses and liverworts. *American Journal of Botany* 86: 1544–1555.
- Tam YY, Epstein E, Normanly J. 2000. Characterization of auxin conjugates in *Arabidopsis*: low steady-state levels of indole-3-acetyl-aspartate, indole-3-acetyl-glutamate, and indole-3-acetyl-glucose. *Plant Physiology* 123: 589–596.
- Tamura K, Stecher G, Peterson D, Filipiński A, Kumar S. 2013. MEGA6: Molecular Evolutionary Genetics Analysis version 6.0. *Molecular Biology and Evolution* 30: 2725–2729.
- Tanaka K, Hayashi KI, Natsume M, Kamiya Y, Sakakibara H, Kawaide H, Kasahara H. 2014. UGT74D1 catalyzes the glucosylation of 2-oxindole-3-acetic acid in the auxin metabolic pathway in *Arabidopsis*. *Plant and Cell Physiology* 55: 218–228.
- Terol J, Domingo C, Talón M. 2006. The GH3 family in plants: genome wide analysis in rice and evolutionary history based on EST analysis. *Gene* 371: 279–290.
- Vanneste S, Friml J. 2009. Auxin: a trigger for change in plant development. *Cell* 136: 1005–1016.
- Westfall CS, Herrmann J, Chen Q, Wang S, Jez JM. 2011. Modulating plant hormones by enzyme action. *Plant Signaling & Behavior* 5: 1607–1612.
- Westfall CS, Sherr AM, Zubieta C, Alvarez S, Schraft E, Marcellin R, Ramirez L, Jez JM. 2016. *Arabidopsis thaliana* GH3.5 acyl acid amido synthetase mediates metabolic crosstalk in auxin and salicylic acid homeostasis. *Proceedings of the National Academy of Sciences, USA* 113: 13917–13922.
- Winter D, Vinegar B, Nahal H, Ammar R, Wilson GV, Provart NJ. 2007. An “electronic fluorescent pictograph” browser for exploring and analyzing large-scale biological data sets. *PLoS ONE* 8: e718.
- Zhang J, Lin JE, Harris C, Campos Mastrotti Pereira F, Wu F, Blakeslee JJ, Peer WA. 2016. DAO1 catalyzes temporal and tissue-specific oxidative inactivation of auxin in *Arabidopsis thaliana*. *Proceedings of the National Academy of Sciences, USA* 113: 11010–11015.
- Zhang J, Peer WA. 2017. Auxin homeostasis: the DAO of catabolism. *Journal of Experimental Botany* 68: 3145–3154.
- Zhao Y. 2018. Essential roles of local auxin biosynthesis in plant development and in adaptation to environmental changes. *Annual Review of Plant Biology* 69: 417–435.
- Zhao Z, Zhang Y, Liu X, Zhang X, Shichang L, Yu X, Ren Y, Zheng X, Zheng X, Zhou K *et al.* 2013. A role for a dioxygenase in auxin metabolism and reproductive development in rice. *Developmental Cell* 27: 113–122.
- Zimin A, Stevens KA, Crepeau MW, Holtz-Morris A, Koriabine M, Marçais G, Puig D, Roberts M, Wegrzyn JL, de Jong P *et al.* 2014. Sequencing and assembly of the 22-Gb loblolly pine genome. *Genetics* 196: 875–890.
- Žizková E, Kubeš M, Dobrev PI, Příbyl P, Šimura J, Zahajská L, Drábková LZ, Novák O, Motyka V. 2017. Control of cytokinin and auxin homeostasis in cyanobacteria and algae. *Annals of Botany* 119: 151–166.

## Supporting Information

Additional Supporting Information may be found online in the Supporting Information section at the end of the article.

**Fig. S1** Full-length coding sequence of *PaGH3.16*, *PaGH3.17*, *PaGH3.gII.8*, *PaGH3.gII.9*, *Pa2OGD.1*, *Pa2OGD.2*, *Pa2OGD.6* and *Pa2OGD.8*.

**Fig. S2** Levels of IAA metabolites in different organs of *Pinus sylvestris* and *Pinus contorta* seedlings.

**Fig. S3** Concentrations of IAA metabolites in different organs of *Picea abies* after feeding with unlabelled IAA.

**Fig. S4** Concentrations of IAA metabolites in *Pinus sylvestris* and *Pinus contorta* roots after feeding with unlabelled IAA.

**Fig. S5** Multiple sequence alignment of predicted amino acid sequences of PaGH3 and AtGH3 proteins.

**Fig. S6** Phylogenetic relationships of GH3 proteins between *Picea abies* and other seed plants.

**Fig. S7** Western blot analysis of IPTG-induced recombinant PaGH3.16, PaGH3.gII.8, PaGH3.gII.9 and PaGH3.17 proteins.

**Fig. S8** Phylogenetic relationships of 2OGD proteins between *Picea abies*, other land plants and chlorophytes.

**Fig. S9** Bacterial assay of IAA oxidation mediated by recombinant Pa2OGD.1, Pa2OGD.2, Pa2OGD.6 and Pa2OGD.8 proteins.

**Table S1** Primers used in this work.

Please note: Wiley Blackwell are not responsible for the content or functionality of any Supporting Information supplied by the authors. Any queries (other than missing material) should be directed to the *New Phytologist* Central Office.